predict small variations in N-H bond lengths in imidazole systems solely from the ^{14}N quadrupole tensor parameters. In addition, the aforementioned opposing changes that occur in the A occupancies of the imino and amino imidazole nitrogens are consistent with the hypothesized decrease in N2-H9 bond length upon copper binding. As the imidazole moiety becomes more negative on going from the protonated to the copper-bound forms, the amino N_δ-H bond lengths become progressively shorter. Thus as the strength of the N-H bond increases, the valence A occupancy decreases and with it a concomitant positive increase in the nitrogen net formal charge.

Conclusions

The hyperfine tensor of the imidazole remote nitrogen of histidine has been accurately determined by ESEEM in Cu(II)-doped L-histidine $HCl \cdot H_2O$ single crystals. The tensor anisotropy exhibits a non-axial form as compared to the axial hyperfine tensor found for the remote nitrogen in Cu(II)-doped zinc(II) bis(1,2-dimethylimidazole) dichloride.[14] Unlike this previous ESEEM study, the nitrogen hyperfine tensor in the Cu(II)-doped L-histidine $HCl \cdot H_2O$ system could be reasonably modeled by a simple multipoint representation of the unpaired electron distribution which is delocalized to a small extent from the metal to the imidazole moiety. It is thus difficult to predict the situations where axial or non-axial hyperfine tensors are expected.

Minor spin delocalization in a Cu^{II}(imidazole)$_4$ complex has been previously inferred from the observation of finite isotropic hyperfine components of the imidazole remote nitrogen (by ESEEM[45] and ENDOR[46]) and protons (by ENDOR[46]) in frozen solution studies. The isotropic component of the nitrogen hyperfine tensor in the present system is only slightly smaller than that recently determined in a single-crystal ESEEM analysis of copper doped into the tetrahedral metal site of zinc(II) bis(1,2-dimethylimidazole) dichloride.[14] It appears that this component of the hyperfine interaction is not as sensitive an indicator of copper coordination geometry, and of the postulated metal unpaired orbital, as in the form of the tensor anisotropy. Future studies of similar systems may help evaluate this hypothesis.

The quadrupole tensor for N2 was likewise determined by the single-crystal ESEEM measurements. A good correlation was found between this tensor orientation and the imidazole geometry. This observation in conjunction with calculated estimates of the hyperfine tensor for both imidazole nitrogens indicate that, upon copper ligation, the imidazole moiety does not distort from its position in the crystal structure[24,25] to a degree that is significant within the accuracy of the ESEEM results.

The variations observed in the quadrupole parameters of the remote nitrogen of imidazole of coordinated histidine derived from ESEEM of frozen solution protein samples have been postulated to be the consequence of intermolecular hydrogen-bonding differences.[9,23f] N—H bond lengths and N—H···O=C distances have been roughly correlated by previous crystallographic analysis.[47] Ab initio calculations have shown that the inequivalence of the two imidazole nitrogens in L-histidine $HCl \cdot H_2O$ may also be a factor in the observed quadrupolar variations.[4] Both intramolecular and intermolecular interactions should affect the remote nitrogen N-H bond length. A linear relationship is found between the A valence population of imidazole amino nitrogens and the inverse cube of the corresponding N-H bond lengths in a series of model compounds. Such an empirical dependence has the potential for deducing the N-H bond lengths in imidazole-containing molecules from the analysis of ^{14}N quadrupole tensor parameters.

Acknowledgment. M.J.C. thanks Dr. Jacqueline Vitali for helpful discussions. This work was supported by U.S.P.H.S. Grants RR-02583 and GM-40168 to J.P.

(45) Mims, W. B.; Peisach, J. *J. Chem. Phys.* **1978**, *69*, 4921.
(46) Van Camp, H. L.; Sands, R. H.; Fee, J. A. *J. Chem. Phys.* **1981**, *75*, 1098.
(47) Traylor, R.; Kennard, O.; Versichel, W. *Acta Crystallogr.* **1984**, *B40*, 280.

Normal Modes and NMR Order Parameters in Proteins

Rafael Brüschweiler[†]

Contribution from the Laboratorium für Physikalische Chemie, ETH Zentrum, 8092 Zürich, Switzerland. *Received December 27, 1991*

Abstract: On the basis of a normal-mode analysis of the protein BPTI, it is demonstrated that the very fast time scale backbone motions with correlation times much faster than 100 ps have a measurable influence on both homonuclear and heteronuclear NMR relaxation rates. Significant differences between classical and quantum statistics are found for heteronuclear relaxation.

1. Introduction

Nuclear magnetic relaxation spectroscopy[1] is one of few experimental sources providing spatially resolved information on sub-nanosecond dynamics of biomolecules in solution. Dipolar relaxation data (T_1, $T_{1\rho}$, T_2, and NOE) of heteronuclear spin pairs, such as ^{13}C-H and ^{15}N-H, are often interpreted using the Lipari-Szabo model,[2] where the motion of the involved internuclear vector is characterized by an internal time scale τ_e, an overall time scale τ_c, and an order parameter S^2. Recently, Clore et al.[3] extended the Lipari-Szabo model by the introduction of an additional order parameter S_f^2, which characterizes the spatial extent of very fast time scale motions ($\tau_e \ll 100$ ps) such as atomic fluctuations and vibrations. The results in ref 3 show that, for most parts of the backbone of the investigated protein (interleukin β), the dominant contribution to the total order parameter S^2 is given by S_f^2 (exceptions are mobile loop regions).

The experimental accessibility of S_f^2 is interesting from a theoretical point of view, since it allows a direct atom-site-specific comparison between analytical as well as force-field-based molecular motional models and NMR data. In the present con-

[†] Present address: Department of Molecular Biology, The Scripps Research Institute, 10666 North Torrey Pines Rd., La Jolla, CA 92037.

(1) Abragam, A. *Principles of nuclear magnetism*; Clarendon Press: Oxford, England, 1961.
(2) Lipari, G.; Szabo, A. *J. Am. Chem. Soc.* **1982**, *104*, 4546.
(3) (a) Clore, G. M.; Szabo, A.; Bax, A.; Kay, L. E.; Driscoll, P. C.; Gronenborn, A. M. *J. Am. Chem. Soc.* **1990**, *112*, 4989. (b) Clore, G. M.; Driscoll, P. C.; Wingfield, P. T.; Gronenborn, A. M. *Biochemistry* **1990**, *29*, 7387.

0002-7863/92/1514-5341$03.00/0

tribution, a description of the order parameters S_f^2 is attempted on the basis of the perhaps simplest detailed motional model, namely a *normal mode analysis* (NMA),[4] applied to the model protein BPTI (basic pancreatic trypsin inhibitor)[5] to study the behavior of theoretical hetero- and homonuclear order parameters along the backbone. Normal modes describe the molecule as a high-dimensional harmonic oscillator, allowing the inclusion of quantum statistics for the treatment of the oscillators coupled to a heat bath. NMA does not access anharmonic and transitional types of protein motion and focuses on the very fast time scale dynamics fulfilling $\tau_e \ll \tau_c$, leading to $(S^2)_{NMA} \cong S_f^2$.

2. Theory

The NMR order parameter S^2 for dipolar relaxation is given by[2]

$$S^2 = \frac{4\pi}{5}\left\langle\frac{1}{r^6}\right\rangle^{-1}\sum_{m=-2}^{2}\left\langle\frac{Y_2^m(\Omega_{mol})}{r^3}\right\rangle\left\langle\frac{Y_2^{m*}(\Omega_{mol})}{r^3}\right\rangle \quad (1)$$

where r is the length, $\Omega_{mol} = (\theta,\varphi)$ is the direction of the vector in a molecule fixed frame connecting the two dipolar interacting spins, and $Y_2^m(\Omega)$ are the spherical harmonics of rank 2. In the following analysis, use is made of the fact that, for both heteronuclear[6] and homonuclear[7] dipolar order parameters, the influences of radial and angular motions can be separated according to

$$S^2 \cong S_\Omega^2 \cdot S_r^2 \quad (2)$$

where

$$S_\Omega^2 = \frac{4\pi}{5}\sum_{m=-2}^{2}\langle Y_2^m(\Omega)\rangle\langle Y_2^{m*}(\Omega)\rangle \qquad S_r^2 = \langle 1/r^3\rangle^2/\langle 1/r^6\rangle$$

S_Ω^2 and S_r^2 are the *angular* and the *radial order parameters*,[7] respectively. The angular brackets in eqs 1 and 2 indicate averaging over the canonical ensemble spanned by the normal modes.

Generally, the normal-mode average[6] of a scalar function $f(\vec{x})$ depending on the $3N$-dimensional space vector $\vec{x}$, where N is the number of atoms in the system fluctuating around the conformational energy minimum $\vec{x}_0$, is up to second-order Taylor expansion

$$\langle f(\vec{x})\rangle \cong f(\vec{x}_0) + \frac{1}{2}\sum_{i=7}^{3N}\sum_{k,l}\frac{\partial^2}{\partial x_k \partial x_l}f(\vec{x}_0)\; m_k^{-1/2} m_l^{-1/2} Q_{i,k} Q_{i,l} \sigma_i^2 \quad (3)$$

where m_k is the mass of the atom belonging to x_k and $Q_{i,k}$ is component k of normal mode $\vec{Q}_i$.[8] The $3N$ normal modes fulfill the equations

$$\mathbf{M}^{-1/2}\mathbf{K}\mathbf{M}^{-1/2}\vec{Q}_i = \omega_i^2\vec{Q}_i \quad (4)$$

$$\vec{Q}_i \cdot \vec{Q}_j = \delta_{ij} \quad (5)$$

where δ_{ij} is the Kronecker symbol and $i, j = 1, \ldots, 3N$. The $3N \times 3N$ matrix $\mathbf{M}$ is diagonal with elements $M_{3k-2,3k-2} = M_{3k-1,3k-1} = M_{3k,3k} = m_k$ ($k = 1, \ldots, N$), and the matrix $\mathbf{K}$ is given by $K_{ij} = (\partial^2/\partial x_i \partial x_j)U(\vec{x}_0)$, where $U(\vec{x}_0)$ is the potential energy function evaluated in the conformational energy minimum $\vec{x}_0$. The sum over i in eq 3 does not include the first six modes ($i = 1, \ldots, 6$) with $\omega_i = 0$ corresponding to the overall translational and rotational degrees of freedom. For the evaluation of the averages in eqs 1 and 2, $k, l = 1, \ldots, 6$, since they involve pairs of atoms defined by 2×3 Cartesian coordinates. The second moments σ_i^2 of the amplitude distributions of the $3N - 6$ independent harmonic oscillators can be calculated according to classical as well as quantum statistics:[9] For the *classical* case

$$\sigma_{i,class}^2 = kT/\omega_i^2 \quad (6)$$

and for the *quantum mechanical* case

$$\sigma_{i,qm}^2 = \frac{h}{4\pi\omega_i}\coth\frac{h\omega_i}{4\pi kT} \quad (7)$$

In the present application the quantum statistic is correct, since normal modes can be considered as phonons which belong to the class of bosons. The two statistics coincide in the limits of low frequency and high temperature, respectively. Using normal-mode calculations, it has been found earlier,[17] for root-mean-square fluctuations of heavy atoms in proteins, that quantum effects are negligible for temperatures above 50 K. The same temperature threshold does not necessarily apply for NMR order parameters involving protons, which are, due to their small mass, characteristically involved in high-frequency modes, as is discussed in the next section.

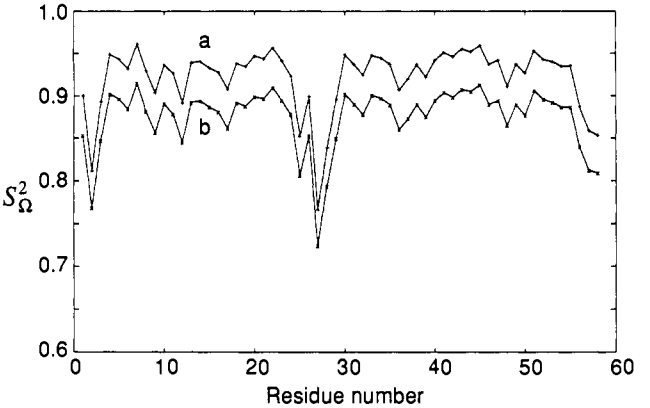

Figure 1. Theoretical heteronuclear angular order parameters S_Ω^2 of C_α–H_α atom pairs of the BPTI backbone calculated from normal modes at $T = 309$ K. The points on curve a correspond to classical statistics, and the ones on curve b, to quantum statistics. For glycine residues (positions 12, 28, 36, 37, 56, 57) the effect of only one H_α is shown.

3. Results and Discussion

3.1. Heteronuclear Relaxation. The normal-mode analysis has been performed on an energy-minimized crystal structure of BPTI including all hydrogen atoms explicitly (904 atoms) using CHARMM[10] with the parameter set PARALLH19. For the subsequent analysis the temperature T has been set to 309 K. The relevance of quantum effects for the heteronuclear case is shown in Figure 1, where the angular order parameters S_Ω^2 of the C_α–H_α pairs are given for classical statistics (a) and quantum statistics (b). Backbone parts with high orientational flexibility (low-order parameters) are found at the beginning and at the end of the polypeptide chain and in the loop region of the antiparallel β-sheet around lysine-26. Quantum statistics leads generally to lower S_Ω^2 and S_r^2, since the spatial probability distribution of the quantum mechanical harmonic oscillator is—as a consequence of the zero-point oscillation—wider than that of the classical one. The systematic difference between the two statistics, which is visible in Figure 1, is between 5% and 6%, i.e. virtually independent of amino acid type and site in the protein. The $S_{\Omega,qm}^2$ values of the C_α–H_α pairs range from 0.72 to 0.92. For each glycine, S_Ω^2 differs for the two H_α protons by less than 1.5%, indicating that the internal dynamics at the corresponding C_α site is governed by motions around axes which are orthogonal to the internuclear $H_{\alpha1}$–$H_{\alpha2}$ vector, such as local backbone dynamics involving the adjacent φ and ψ dihedral angles.

(4) (a) Wilson, E. B., Jr.; Decius, J. C.; Cross, P. C. *Molecular vibrations*; McGraw-Hill: New York, 1955. (b) Noguti, T.; Gō, N. *J. Phys. Soc. Jpn.* **1983**, *52*, 3283, 3685. (c) Brooks, B. R.; Karplus, M. *Proc. Natl. Acad. Sci. U.S.A.* **1983**, *80*, 6571. (d) Levitt, M.; Sander, C.; Stern, P. S. *J. Mol. Biol.* **1985**, *181*, 423. (e) Roux, B.; Karplus, M. *Biophys. J.* **1988**, *53*, 297. (f) Smith, J.; Cusack, S.; Tidor, B.; Karplus, M. *J. Chem. Phys.* **1990**, *93*, 2974. (g) Kottalam, J.; Case, D. A. *Biopolymers* **1990**, *29*, 1409.

(5) (a) Deisenhofer, J.; Steigemann, W. *Acta Crystallogr., Sect. B* **1975**, *31*, 238. (b) Walter, J.; Huber, R. *J. Mol. Biol.* **1983**, *167*, 911. (c) Richarz, R.; Nagayama, K.; Wüthrich, K. *Biochemistry* **1980**, *19*, 5189. (d) Ribeiro, A. A.; King, R.; Restivo, C.; Jardetzky, O. *J. Am. Chem. Soc.* **1980**, *102*, 4040. (e) Lipari, G.; Szabo, A. *J. Am. Chem. Soc.* **1982**, *104*, 4559. (f) van Gunsteren, W. F.; Karplus, M. *Biochemistry* **1982**, *21*, 2259. (g) Nirmala, N. R.; Wagner, G. *J. Am. Chem. Soc.* **1988**, *110*, 7557.

(6) Henry, E. R.; Szabo, A. *J. Chem. Phys.* **1985**, *82*, 4753.

(7) (a) Brüschweiler, R. Structural dynamics in biomolecules monitored by NMR relaxation. Thesis No. 9466, ETH Zürich, 1991. (b) Brüschweiler, R.; Roux, B.; Blackledge, M.; Griesinger, C.; Karplus, M.; Ernst, R. R. *J. Am. Chem. Soc.*, in press.

(8) Goldstein, H. *Classical mechanics*; Addison-Wesley: Reading, MA, 1981.

(9) Landau, L. D.; Lifschitz, E. M. *Lehrbuch der theoretischen Physik, Statistische Mechanik*; Akademie-Verlag: Berlin, 1976.

(10) Brooks, B. R.; Bruccoleri, R. E.; Olafsen, B. D.; States, D. J.; Swaminathan, S.; Karplus, M. *J. Comput. Chem.* **1983**, *4*, 187.

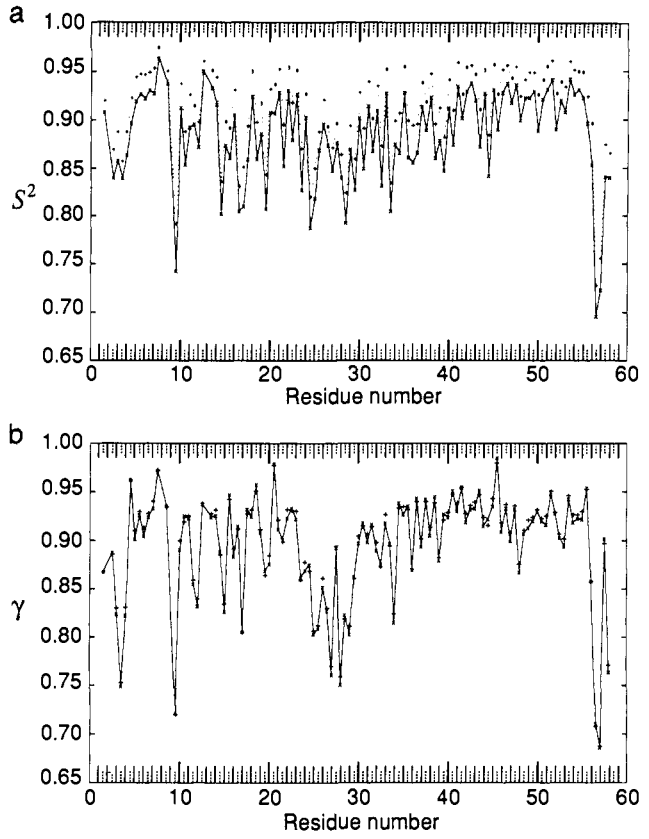

Figure 2. Effect of normal modes on homonuclear order parameters. (a) S^2 for intraresidual NH(i)-H$_\alpha$(i) and sequential H$_\alpha$(i)-NH(i+1) NOE/ROEs. The intraresidual NH(i)-H$_\alpha$(i) pairs (i = amino acid number) are given at the solid tick-mark positions and the sequential H$_\alpha$(i)-NH(i+1) pairs at the dotted tick-mark positions. The classical order parameters (+) are connected by the dotted line, and the order parameters calculated with quantum statistics (×) are connected by the solid line. In the case of a proline at position i, S^2 is given for the pairs H$_\alpha$(i-1)-H$_\alpha$(i) and H$_\alpha$(i)-NH(i+1). (b) Ratio γ between dynamic and static NOE/ROEs for the same proton pairs shown in (a). The solid line connects γ calculated with quantum statistics (×), and the + symbols refer to classical statistics.

For isotropic overall rotational tumbling, the relative dependence of heteronuclear T_1, $T_{1\rho}$, and T_2 relaxation rates on the statistics is the same and can be expressed by the ratio α

$$\alpha = \frac{(1/T_{1,1\rho,2})_{qm}}{(1/T_{1,1\rho,2})_{class}} = \frac{S^2_{\Omega,qm}\langle r^{-3}\rangle^2_{qm}}{S^2_{\Omega,class}\langle r^{-3}\rangle^2_{class}} \tag{8}$$

which lies between 0.95 and 0.96 for the C$_\alpha$-H$_\alpha$ pairs. For backbone N-H pairs, α ranges from 0.91 to 0.93. Therefore, a fully quantitative interpretation of measured order parameters on the basis of a classical motional model, such as an MD simulation, can be inadequate. It is conceivable to correct classically simulated relaxation parameters for vibrational quantum effects a posteriori. It should be noted that the heteronuclear NOE,[11] which is essentially a ratio of two relaxation rates, does not depend on the fast time scale motions considered here.

Although the conformational space sampled by the normal modes is limited to the harmonic neighborhood of a single structure, the induced orientational disorder has a remarkable effect on the relaxation rates. Therefore, the interpretation of more complex experimental relaxation data originating from a superposition of slow (transitional) *and* fast (vibrational) time scale motions will benefit from a realistic picture of the influence of the omnipresent fast time scale molecular dynamics.

3.2. Homonuclear Cross Relaxation. Homonuclear proton-proton cross relaxation as measured via NOESY and ROESY

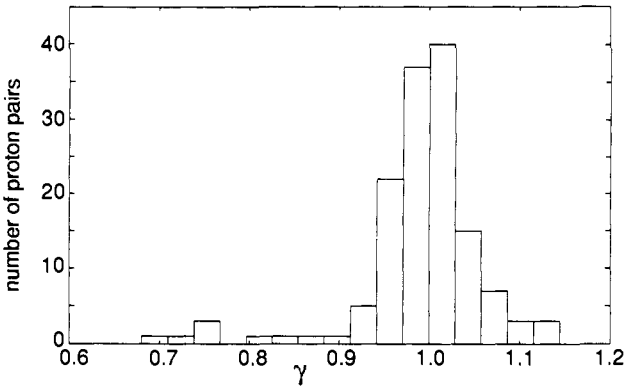

Figure 3. Distribution of the dynamic scaling factor γ (see eq 9) for long-range NOE/ROEs involving NH, H$_\alpha$, or H$_\beta$ protons (141 proton pairs). Long-range NOE/ROEs are separated by more than five residues in primary sequence. The proton-proton distance cutoff is set to 4.5 Å.

experiments[12] differs from heteronuclear relaxation with respect to the lattice by the facts that the interacting nuclei have much larger average distances $\langle r\rangle > 1.7$ Å and that they are separated by at least one (mobile) dihedral angle (except geminal proton pairs). Sequential intraresidual and interresidual backbone-backbone NOEs and ROEs (NOE/ROEs) associated with the proton pairs NH(i)-H$_\alpha$(i) and H$_\alpha$(i)-NH(i+1) (i indicates the amino acid position in the primary sequence) are crucial for resonance assignments as well as the characterization of φ and ψ backbone dihedral angles.[13] The corresponding order parameters S^2 are given in Figure 2a. The difference between quantum and classical statistics is clearly smaller than in the case of directly bonded heteronuclear spin pairs. S^2 is a collective measure for the spatial restriction of the corresponding internuclear vector and ranges between 0.69 and 0.97. Angular and radial disorders both lead to a reduction of S^2. However, S^2 is not directly observable, and it is the competitive interference of angular and radial disorders which determines the magnitude of the cross-relaxation rate. Comparison with Figure 1 shows that there is no conspicuous relationship between heteronuclear and homonuclear order parameters having a proton in common.

Internal molecular motions with correlation times much faster than $1/\omega_0$, such as normal-mode dynamics, scale NOESY and ROESY cross-relaxation rates by the same factor γ[7]

$$\gamma = \frac{\Gamma^{NOE/ROE}_{dyn}}{\Gamma^{NOE/ROE}_{stat}} = \langle r\rangle^6\left\langle\frac{1}{r^6}\right\rangle S^2 \tag{9}$$

where $\Gamma^{NOE/ROE}_{dyn}$ corresponds to the dynamically averaged rate and $\Gamma^{NOE/ROE}_{stat}$ to the rate calculated from the static structure. Figure 2b shows γ for the same proton pairs given in Figure 2a. The general decrease of the cross-relaxation rates ($\gamma < 1$) reflects the dominance of angular over radial fluctuations for these short-range proton pairs. The motional "quenching" can be as strong as 70%, corresponding to the rate of a static pair with a 6% longer internuclear distance. This error is sufficiently small to be irrelevant for the generation of an averaged protein conformation on the basis of NMR distance constraints. However, structural refinement procedures involving back-calculation of the cross-relaxation rates[14] might be affected. Figure 2b also illustrates the dependence of γ on the nature of the applied statistics: The γ values calculated for quantum statistics (×) and classical statistics (+) are very

(11) Noggle, J. H.; Schirmer, R. E. *The nuclear Overhauser effect, chemical applications*; Academic Press: New York, 1971.

(12) (a) Ernst, R. R.; Bodenhausen, G.; Wokaun, A. *Principles of nuclear magnetic resonance in one and two dimensions*; Clarendon Press: Oxford, England, 1987. (b) Bothner-By, A. A.; Stephens, R. L.; Lee, J.; Warren, C. D.; Jeanloz, R. W. *J. Am. Chem. Soc.* **1984**, *106*, 811.

(13) Wüthrich, K. *NMR of proteins and nucleic acids*; Wiley-Interscience: New York, 1986.

(14) (a) Boelens, R.; Koning, T. M. G.; van der Marel, G. A.; van Boom, J. H.; Kaptein, R. *J. Magn. Reson.* **1989**, *82*, 290. (b) Yip, P.; Case, D. A. *J. Magn. Reson.* **1989**, *83*, 643. (c) Borgias, B. A.; Gochin, M.; Kerwood, D. J.; James, T. L. *Prog. Nucl. Magn. Reson. Spectrosc.* **1990**, *22*, 83. (d) Mertz, J. E.; Güntert, P.; Wüthrich, K.; Braun, W. *J. Biomol. NMR* **1991**, *1*, 257.

similar (difference <1%), since the larger spatial separation compared to the heteronuclear case reduces the effect of vibrational high-frequency modes. Hence, the averaging is dominated by more collective (low-frequency) motions, which are rather insensitive to the type of statistics. This means that, for the considered proton pairs, MD simulations and NMA give equivalent results on the influence of vibrational dynamics on cross relaxation.

The distribution of γ for *long-range backbone NOE/ROEs* is given in Figure 3. The centering of γ around 1.0 indicates an increased weight of radial fluctuations compared to the angular ones. Hence, the structurally important long-range NOE/ROEs are on average rather weakly perturbed by the normal-mode dynamics. On the other hand, geminal proton pairs, such as $H_{\beta 1}$-$H_{\beta 2}$ and $H_{\alpha 1}$-$H_{\alpha 2}$ (glycines), have γ values distributed around 0.8 (not shown). Consequently, their use for distance calibration tends to bias the long-range distances toward values that are slightly too small (around 4%) and corrects at the same time for the motionally scaled short-range NOE/ROEs of Figure 2, provided that the dominant dynamics lie in the fast time scale regime. The difference for γ between classical and quantum statistics becomes larger for geminal proton pairs but still remains below 3%.

4. Conclusion

The results presented here demonstrate for the protein BPTI that the very fast time scale motions, represented by normal modes, can have a considerable influence on both hetero- and homonuclear relaxation rates. This is consistent with experimental results obtained for other proteins.[3,15] A non-negligible difference of 4%-5% between quantum and classical statistics is found for heteronuclear C_α-H_α relaxation. This effect is to be considered and should be corrected for in the interpretation of heteronuclear relaxation data using classical simulations. Comparison between measured and calculated order parameters allows tests and eventual refinements of biomolecular force fields and might support the development of potentials of mean force to mimic solvent effects.[16] The influence of vibrational motions on averaged internuclear distances extracted from proton cross-relaxation data is small and should become noticeable only for the generation of very high resolution protein structures.

Acknowledgment. Dr. Benoit Roux is thanked for helpful discussion, Zoltan Mâdi for porting CHARMM to a Convex C2, and Prof. Dr. Richard R. Ernst for encouragement, discussion, and support. This work was financially supported by the Swiss National Science Foundation.

Registry No. BPTI, 9087-70-1.

(15) (a) Kay, L. E.; Torchia, D. A.; Bax, A. *Biochemistry* **1989**, *28*, 8972. (b) Palmer, A. G.; Rance, M.; Wright, P. E. *J. Am. Chem. Soc.* **1991**, *113*, 4371.

(16) McQuarrie, D. A. *Statistical mechanics*; Harper & Row: New York, 1976.

(17) Brooks, C. L., III; Karplus, M.; Pettitt, B. M. *Proteins: A theoretical perspective of dynamics, structure, and thermodynamics*; John Wiley and Sons: New York, 1987.

How "Stable" Is Cyclobutyne? The Activation Energy for the Unimolecular Rearrangement to Butatriene

Heather A. Carlson,† Geoffrey E. Quelch, and Henry F. Schaefer III*

Contribution from the Center for Computational Quantum Chemistry, University of Georgia, Athens, Georgia 30602. *Received June 28, 1991*

Abstract: The barrier height for the disappearance of the singlet ground state of cyclobutyne has been investigated using ab initio molecular quantum mechanical methods. Stationary-point geometries were determined using the two-configuration self-consistent-field (TCSCF) method in conjunction with double zeta plus polarization (DZP) basis sets. The transition state exhibits strong biradical behavior. At the DZ+P TCSCF level, the classical barrier for unimolecular rearrangement to butatriene is 55 kcal/mol. With configuration interaction including all single and double excitations with respect to both TCSCF reference configurations, the classical barrier is reduced to 51 kcal/mol. Significant further lowerings in the cyclobutyne barrier occur when coupled cluster (CC) methods are applied. Including all connected triple excitations with the CCSD(T) method, the classical barrier is reduced to 41 kcal/mol with the DZP basis. Further corrections for the inherent "two reference configuration" nature of the problem and for zero-point vibrational energy yield a final value of ~25 kcal/mol for the activation energy. Thus clyclobutyne is reasonably stable with respect to unimolecular isomerization to butatriene.

Introduction

A question of long-standing interest[1-24] in physical organic chemistry is: "What is the smallest otherwise saturated cyclic hydrocarbon that can accommodate a C≡C triple bond?" Experimentally, the smallest cycloalkyne that has been spectroscopically identified appears to be cyclohexyne, for which Wentrup, Blanch, Briehl, and Gross[22] recently assigned the C≡C triple bond stretch to an infrared feature in the range 2090-2105 cm^{-1}. For cyclopentyne, Miller and Chapman[23] have very tentatively suggested that cyclopentyne may be the carrier of an infrared spectrum characterized by two strong bands at 2125 and 2077 cm^{-1}, a band of medium intensity at 1646 cm^{-1}, and two weak bands at 908 and 627 cm^{-1}. Experimental studies of cyclobutyne and its derivatives have proven to be inconclusive.[1,2]

† CCQC Summer Undergraduate Fellow from North Central College, Naperville, IL.

(1) Montgomery, L. K.; Roberts, J. D. *J. Am. Chem. Soc.* **1960**, *82*, 4750.
(2) Wittig, G.; Wilson, E. R. *Chem. Ber.* **1965**, *98*, 451.
(3) Montgomery, L. K.; Scardiglia, F.; Roberts, J. D. *J. Am. Chem. Soc.* **1965**, *87*, 1917.
(4) Hoffmann, R. W. *Dehydrobenzene and Cycloalkynes*; Academic Press: New York, 1967.
(5) Krebs, A. *Chemistry of Acetylenes*; Viehe, H. G., Ed.; Marcel Dekker: New York, 1969; pp 987-1062.
(6) Nakagawa, M. *The Chemistry of the Carbon-Carbon Triple Bond*; Patai, S., Ed.; Wiley: Chichester, England, 1978; pp 635-712.
(7) Greenberg, A.; Liebman, J. F. *Strained Organic Molecules*; Academic Press: New York, 1978; pp 133-138.
(8) Chapman, O. L. Cope Award Lecture, 176th National Meeting of the American Chemical Society, Miami Beach, FL, Sept 1978. A semipopular account of this lecture was given in: *Chem. Eng. News* **1978**, No. 17, 18.

0002-7863/92/1514-5344$03.00/0